On Mathematical Models of Two-Minute Stereoscopic Viewing on Human Balance Function

Fumiya Kinoshita[1,2*], Yuki Mori[2], Masaru Miyao[1] and Hiroki Takada[2]

[1]*Department of Information Engineering, Graduate School of Information Science, Nagoya University, Furo-cho, Nagoya 464-8603, Japan*
[2]*Department of Artificial Inteligence, University of Fukui, 3-9-1 Bunkyo, Fukui 910-8507, Japan*
**E-mail address: kinoshita.fumiya@j.mbox.nagoya-u.ac.jp*

(Received April 30, 2015; Accepted December 1, 2015)

In contrast to two-dimensional (2D) films that project flat images, stereoscopic films elicit the feeling of being at a live performance. However, asthenopia and visually-induced motion sickness (VIMS) can result from the exposure to these films. Even though various hypotheses exist, the pathogenesis of VIMS is still unclear. There is not enough knowledge on the effects of stereoscopic images on the living body, and the accumulation of basic research is thus important. The aim of this paper is to accumulate information relevant to VIMS and to examine whether the exposure to 3D video clips affects the human equilibrium functions. We also verified that 3D viewing effects on our equilibrium function depends on exposure time.
Key words: Visually Induced Motion Sickness, Stabilometry, Stereoscopic Image, Stochastic Differential Equation

1. Introduction

Recently, with the rapid progress in image processing and three-dimensional (3D) technologies, stereoscopic images are not only available on television but also in theaters, on game machines, and elsewhere. Current 3D display mechanisms include stereoscopy, integral photography, the differential binocular vision method, volumetric display [1], and holography [2]. Viewing stereoscopic images may elicit adverse effects, such as asthenopia or visually-induced motion sickness (VIMS) in some individuals [3]. While the symptoms of general motion sickness include dizziness and vomiting, the phenomenon of VIMS is not fully understood. Currently, there is not enough knowledge accumulated on the effects of stereoscopic images on the living body and basic research is thus important [4].

At present, VIMS is explained by the sensory conflict theory [5]. In humans, the standing posture is maintained by the body's balance function that is an involuntary physiological adjustment mechanism referred to as the "righting reflex". In order to maintain the standing posture in the absence of locomotion, the righting reflex is initiated in the following sensory system and processed in the nucleus ruber. Sensory receptors, such as visual inputs, auditory and vestibular functions, and proprioceptive inputs from the skin, muscles, and joints, are refered to maintain the body's balance function [6]. According to the sensory conflict theory, motion sickness is a response to the conflict generated by a discrepancy between received and previously stored messages. Variations are thus expected that may arise from acquired experiences. Contradictory messages originating from different sensory systems, or the absence of a sensory message that is expected in a given situation, are thought to lead to the feeling of sickness. Self-spatial localization becomes unstable and produces discomfort. Researchers generally agree that there is a close relationship between the vestibular and autonomic nervous systems both anatomically and electrophysiologically. This view strongly indicates that the equilibrium system is associated with the symptoms of motion sickness [7] and provides a basis for the quantitative evaluation of motion sickness based on body sway, an output of the equilibrium system.

Stabilometry is a useful test of body equilibrium for investigating the overall equilibrium function. Stabilometry methods are presented in the standards of the Japanese Society for Equilibrium Research and in international standards [8]. Stabilometry is a simple test in which 60 seconds recording starts when body sway stabilizes [9]. Objective evaluation is possible by the computer analysis of the speed and direction of the sway, enabling diagnosis of a patient's condition [10].

In previous studies, viewing 3D video clip has been shown to affect body sway [11]. However, thus far, it has not been mentioned on remarkable influence while viewing 3D video clips. In this paper, we examined the 3D video clip effect on our equilibrium function to determine whether it is dependent on the exposure time.

2. Enpirical Study with Stabilometry

2.1 Materials and methods

Sixteen healthy male subjects (mean age ± standard deviation: 22.2 ± 0.7 years) participated voluntarily in the study. We ensured that the body sway was not affected by environmental conditions. We used an air conditioner to adjust the temperature at 25°C in the exercise room.

doi:10.5047/forma.2017.s003

Fig. 1. The video clip shown to the subjects on a 3D display.

The experiment was explained to all subjects and written informed consent was obtained in advance.

In this experiment, we conducted a stabilometry test with subjects viewing 2D and 3D video clips. The device used was a Wii Balance Board (Nintendo, Kyoto). The sampling frequency of the Wii Balance Board was 20 Hz. The subjects stood upright on the device in Romberg's posture. We conducted two types of measurements: (I) after resting for 30 seconds, the body sway of each subject was measured for 1 minute with opened eyes, and (II) after resting for 30 seconds, the body sway of each subject was measured for 2 minutes with opened eyes. We herein collected data for the later half of this 2 minutes. Experiments were performed in a dark room to avoid irritation from sources other than the video. The 2D or 3D video clips were shown on a 3D KDL 40HX80R display (SONY, Tokyo) placed 2 meters away from the subject. In the video clip used in the experiment, while sphere moved around the screen (Fig. 1). A comparison was then made with subjects who were asked to simply gaze at a point 2 meters in front of them. The experiments were carried out in random order. Each experiment was carried out on a separate day.

2.2 Analysis method

The x-y coordinates were recorded for each sampled time point collected in the tests that were conducted with open and closed eyes, and the quantitative indices were calculated. The data were converted to time series and included the position of the center of pressure (COP) in the x (the right direction, designated as positive) and y (the anterior direction, designated as positive) directions in each of the open eye tests. The area of sway, total locus length used for subsequent evaluation. The area of sway and total locus length are analytical indices of stabilograms that were used in previous studies. We used these based on the definitions established by the Japanese Society for Equilibrium Research.

- Area of sway: Area of a region surrounded (enveloped) by the circumferential line of sway on the x-y coordinates. An increase in the value represents a more unstable sway;
- Total locus length: Total extended distance of movement of the COP within the measurement time period. An increase in the value represents a more unstable sway.

The area of sway and total locus length are analytical indices of stabilograms that were used in previous studies. We used these based on the definitions established by the Japanese Society for Equilibrium Research. We calculated the correlation coefficients between the two analysis, respectively.

2.3 Numerical analysis

In stabilogram, variables x (the right direction, designated as positive) and y (the anterior direction, designated as positive) are regarded to be independent [12]. The linear stochastic differential equation (Brownian motion process) have been proposed as a mathematical model to describe body sway [13, 14, 15]. To describe the individual body sway, we especially show that it is necessary to extend the following nonlinear stochastic differential equations:

$$\frac{\partial x}{dt} = -\frac{\partial}{\partial x}U_x(x) + \mu_x w_x(t), \quad (1)$$

$$\frac{\partial y}{dt} = -\frac{\partial}{\partial y}U_y(y) + \mu_y w_y(t), \quad (2)$$

where $w_x(t)$ and $w_y(t)$ are pseudorandom numbers produced by white Gaussian noise [16]. The following formula describes the relationship between the distribution in each direction, $G_x(x)$ and $G_y(y)$ and the temporal averaged potential constituting the stochastic differential equations (SDEs);

$$U_x(x) = -\frac{\mu_x^2}{2}\ln G_x(x) + const., \quad (3)$$

$$U_y(y) = -\frac{\mu_y^2}{2}\ln G_y(y) + const. \quad (4)$$

The variance of stabilograms generally depends on the temporal averaged potential function (TAPF) with several minimum values when it follows the Markov process without abnormal dispersion. SDEs can represent movements within local stability with a high frequency component near the minimal potential surface, where a high density at the measurement point is expected.

Histograms of the stabilograms were obtained from each subjects. Mean of each stabilogram was set to be (0, 0) by statistical processing. We compared histograms that were composed of all subjects' stabilograms with eyes open. The TAPFs in viewing 2D and 3D video clips were determined from the histograms using Eqs. (5) and (6). The TAPFs were herein regressed by the following polynomial of degree 4 (Fig. 2).

$$\widehat{U_x}(x) = a_x x^4 + b_x x^3 + c_x x^2 + d_x x \quad (5)$$

$$\widehat{U_y}(y) = a_y y^4 + b_y y^3 + c_y y^2 + d_y y. \quad (6)$$

The following SDEs were derived from the mathematical model of the body sway Eqs. (1) and (2) into which was substituted the Eqs. (5) and (6).

$$\frac{\partial x}{dt} = -(4a_x x^3 + 3b_x x^2 + 2c_x x + d_x) + \mu_x w_x(t) \quad (7)$$

$$\frac{\partial y}{dt} = -(4a_y y^3 + 3b_y y^2 + 2c_y y + d_y) + \mu_y w_y(t) \quad (8)$$

where μ represents the noise amplitude. We rewrote Eqs. (7) and (8) into the difference equation and obtained numerical solutions with the Runge-Kutta-Gill formula as the

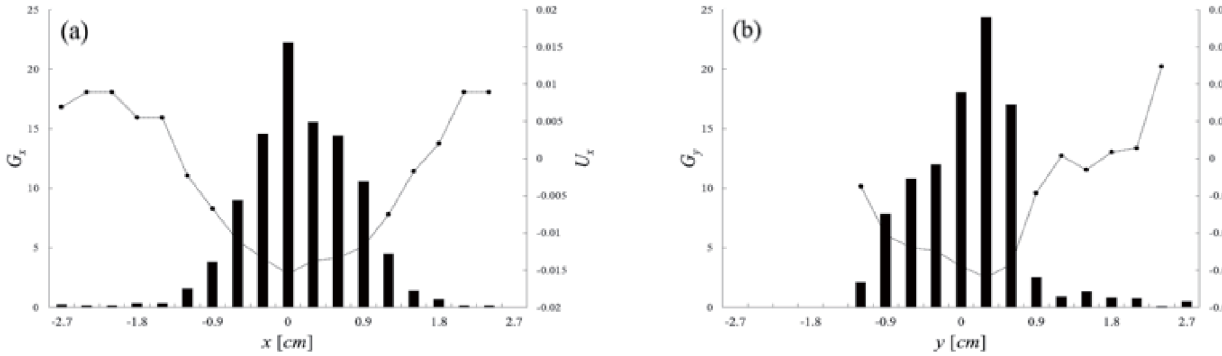

Fig. 2. A typical example of TAPF derived from stabilograms during exposure to the video clip (I)-3D: x directions (a), y directions (b).

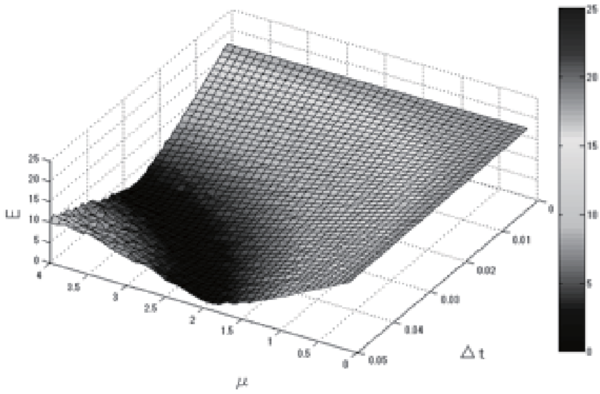

Fig. 3. A typical evaluation for numerical solutions in space spand by the parameter μ and Δt at control.

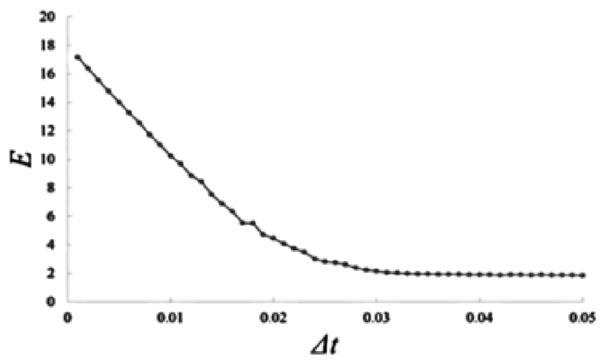

Fig. 4. A typical example of E-Δt plane at control.

numerical calculus. In Eqs. (7) and (8), the initial values of (x, y) were set to be $(0, 0)$. The pseudorandom numbers (mean $\pm$ standard deviation: 1 ± 1) were generated to substitute into the white Gaussian noise w. Setting the noise amplitude μ and time step Δt were set to be every 0.1 step from 0.1 to 4 and 0.001 step from 0.001 to 0.05, respectively. Numerical analysis was employed for 22,000 steps, and the first 10,000 steps of the numerical solutions were discarded due to dependence of the initial value. The remaining 12,000 steps were divided into 1,200-step increments. The area of sway (Ys) and total locus length (Xs) were also calculated in these numerical solutions. Designating the measured the area of sway and the total locus length as (Yr) and (Xr), errors (E) between the numerical solutions of the mathematical model and measured data was defined as follows:

$$E = \sqrt{\frac{\sqrt{Yr}}{Xr}(Xr - Xs)^2 + \left(\sqrt{Yr} - \sqrt{Ys}\right)^2}. \quad (9)$$

We then estimated the smallest E for each parameter μ and Δt (Fig. 3), and the variance of E on E-Δt plane as

$$var(\Delta t^*) = \frac{1}{\#data} \sum_{\Delta t^* \leq \Delta t \leq 0.05} \{E(\Delta t) - mean(E)\}^2, \quad (10)$$

was calculated to determine the plateau of the error E. The left bound Δt^* was defined as the optimum value for the plateau in the case that the variance (10) exceeded 0.3 in this study (Fig. 4). This parameter was calculated for each subject.

3. Results

Stabilograms measured during exposure to a 2D video clip were compared with those of a 3D (Fig. 5). In these figures, the vertical axis shows the anterior and posterior movements of the COP, and the horizontal axis shows the right and left movements of the COP. We also calculated the area of sway, total locus length for each stabilogram (Fig. 6). Regardless of the solidity on video clips (2D/3D), the area of sway and total locus length while viewing video clips (II) were smaller than those while viewing video clips (I), respectively. As a result of the Wilcixon signed-rank test, the value of the area of sway and the total locus length were significantly greater while viewing the video clip (I)-2D and the control compared with those while viewing the video clip (II)-3D ($p < 0.05$).

Histograms of each component were obtained from subjects's stabilograms. The TAPFs in each case (I) and (II) were constructed from the histograms using Eqs. (5) and (6). The TAPFs were sufficiently regressed by those polynomials for degree 4. Eqs. (7) and (8) were rewrote into the difference equation, and the numerical solutions were obtained with the Runge-Kutta-Gill formulae (Fig. 7). The area of sway and total locus length were also calculated in these numerical solutions. The smaller E we obtained, the better description the numerical simulation could give us.

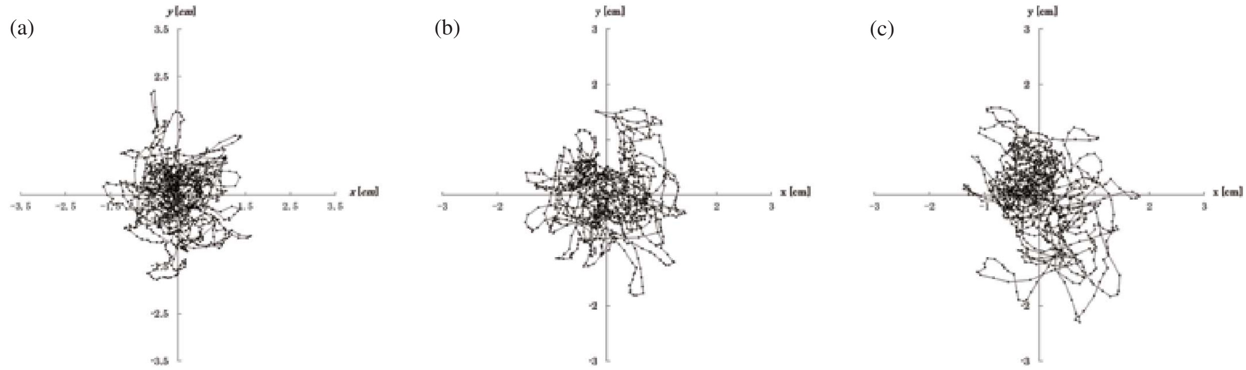

Fig. 5. Typical stabilograms recorded for 1 minute exposure to visual images (I): Control (a); a 2D (b); a 3D (c).

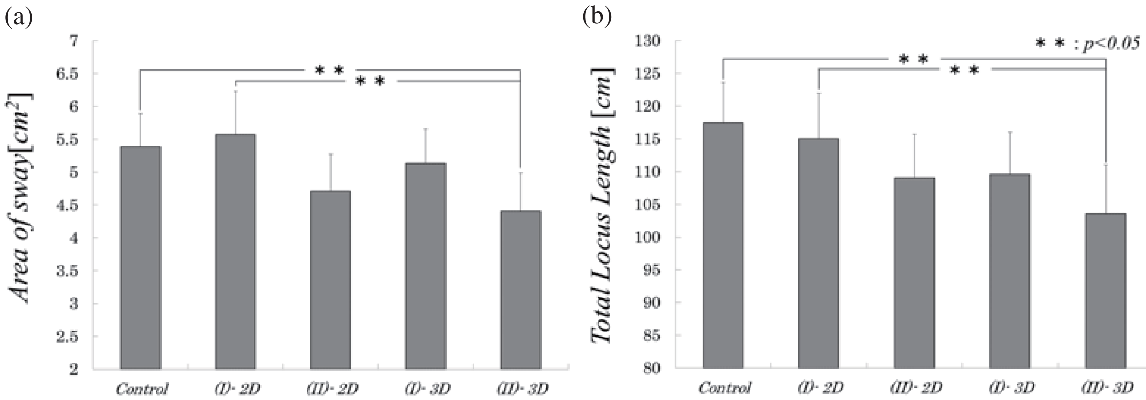

Fig. 6. Result of the area of sway (a) and total locus length (b) (average $\pm$ SE).

The value of errors E was evaluated with the control parameter Δt and μ in the abovementioned difference equations (Fig. 8).

Thereafter we estimate the smallest E for each parameter Δt and μ. The left bound Δt^* was defined as the optimum value for the plateau in the case that the variance (10) exceeded 0.3 in this study. This parameter was calculated for each subject and experimental condition.

The average value of the optimum values is shown in Table 1. The greatest Δt^* was obtained during the control (Fig. 9b). Conversely, the smallest one was obtained while viewing the video clip (II)-3D. The greatest μ was also obtained while viewing the video clip (II)-3D, and the smallest one was obtained while viewing the video clip (I)-2D (Fig. 9a). In this paper, $\mu \times \Delta t^*$ was evaluated for the rigidity of the postural control. The value of $\mu \times \Delta t^*$ while viewing the video clip (II)-3D was smaller than the other case (Fig. 9d). The value while viewing the video clip (II)-3D was significantly smaller than that while viewing the video clip (II)-2D and the control ($p < 0.05$).

4. Discussion

In this paper, we evaluated the body sway during 2D/3D video clips viewing. From the numerical analysis the SDEs (7) and (8), we obtained the smallest rigidity in the postural sway while viewing the video clip (II)-3D. The optimum values in the numerical evaluation were correlated with the sway values. It seems that the optimum noise ampritudes and time step strongly affect the system to control the upright posture. Using the optimum time step Δt^*, we could detect more differences between the condition levels as shown in Fig. 9b. Using a mathematical model for the evaluation of the stabilograms may contribute to the elucidate of the postural control system.

The human standing posture is controled by the equilibrium function, which is involuntary physiological adjustment mechanism. Sensory signals such as visual inputs, auditory/vestibular inputs, and proprioceptive inputs from the skin, muscles, and joints are the inputs that involved in the equilibrium function. It is there is a close relationship between the vestibular and autonomic nervous systems both anatomically and electrophysiologically. This view strongly indicates that the equilibrium system is associated with the symptoms of motion sickness [7] and provides a basis for the quantitative evaluation of motion sickness based on body sway, an output of the equilibrium system. In general, the stabilometry is a simple test for 60 seconds recording after the upright posture was stabilized. It is able to evaluate objectively by the computer analysis of the speed and direction of the body sway, which enables to diagnose and/or follow a patient's condition.

Previous studies have measured the body sway dur-

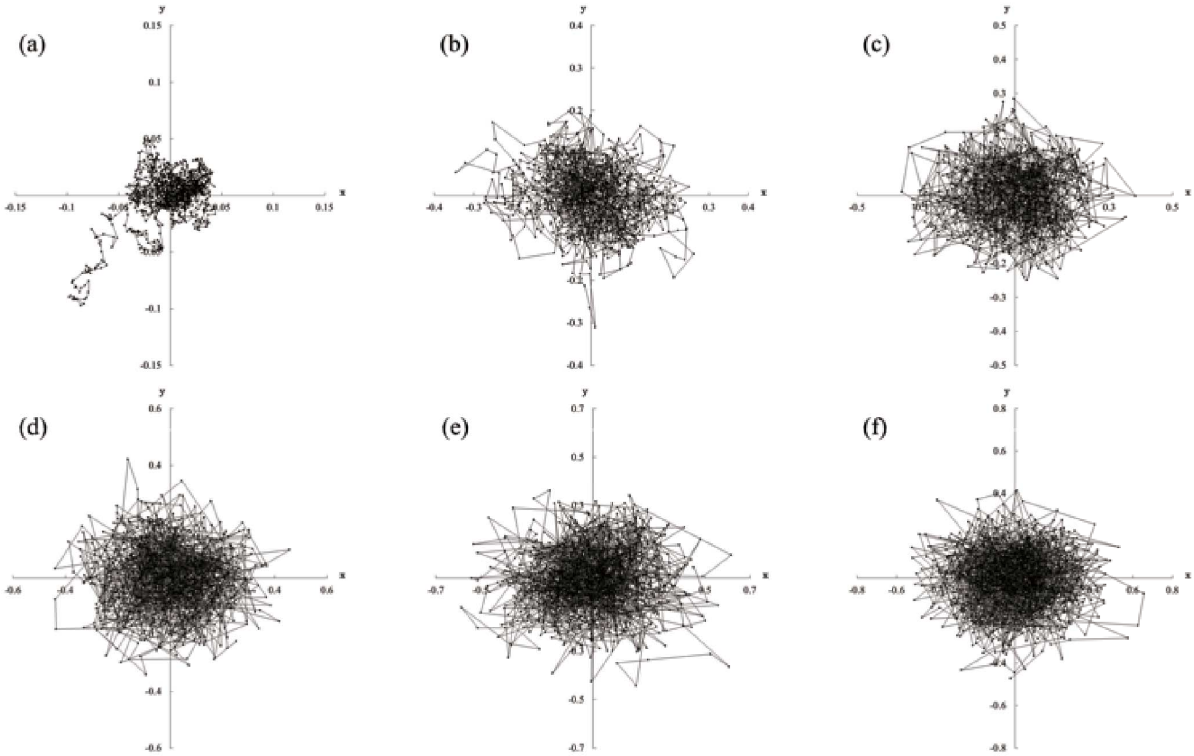

Fig. 7. Typical examples of numerical solutions at $\mu = 3.8$ and the following time step: $\Delta t = 0.001$ (a); $\Delta t = 0.01$ (b); $\Delta t = 0.02$ (c); $\Delta t = 0.03$ (d); $\Delta t = 0.04$ (e); $\Delta t = 0.05$ (f).

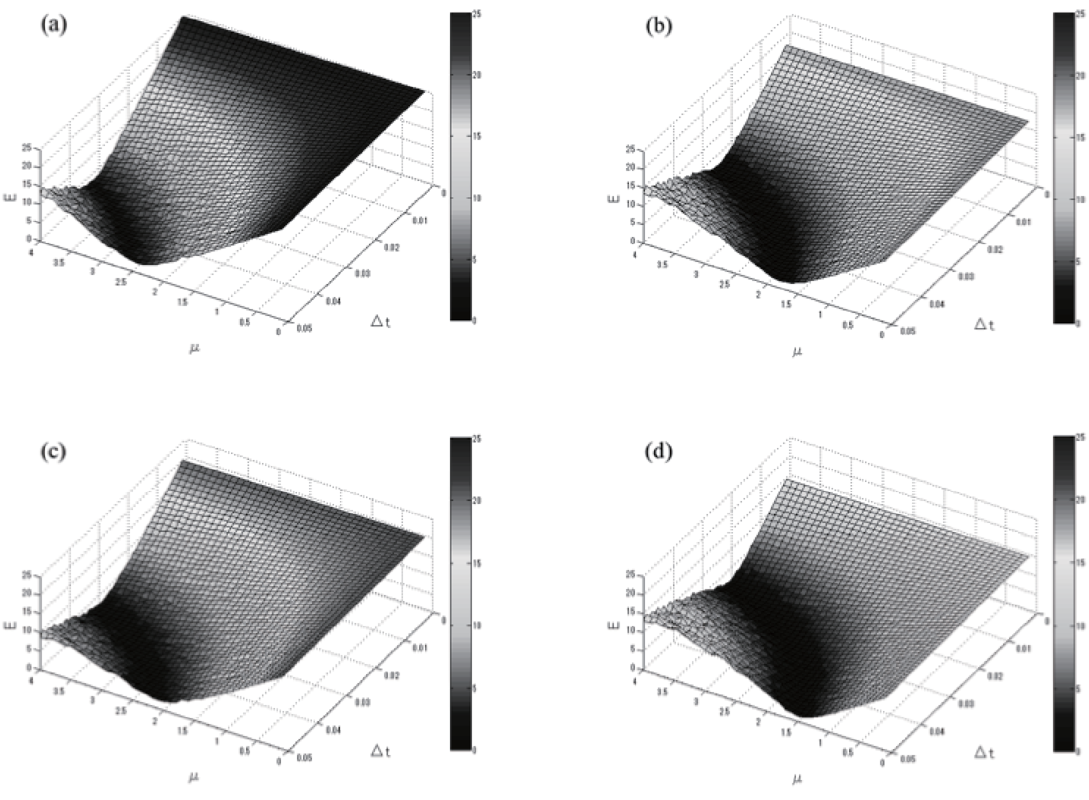

Fig. 8. A typical evaluation for numerical solutions of the mathematical model while viewing the video clip: (I): a 2D (a); (II): a 2D (b); (I): a 3D (c); (II): a 3D (d).

Table 1. Optimum value of numerical solutions (average).

	Control	*(I) - 2D*	*(II) - 2D*	*(I) - 3D*	*(II) - 3D*
Δt^*	0.019	0.019	0.018	0.018	0.017
E	2.915	2.687	2.568	2.694	2.575
μ	3.953	3.927	3.933	3.967	3.993
$\mu \times \Delta t^*$	0.077	0.076	0.072	0.070	0.067

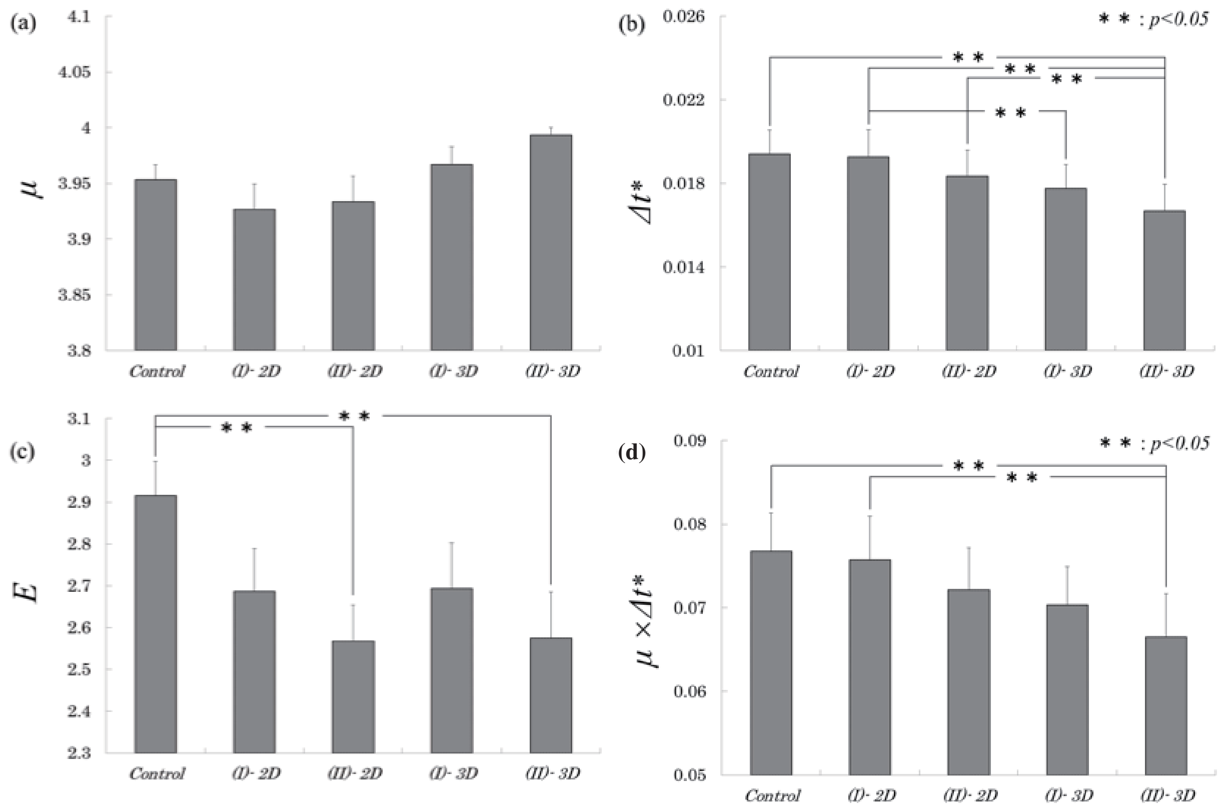

Fig. 9. Results of optimum value (average ± SE): μ (a); Δt^* (b); E (c); $\mu \times \Delta t^*$ (d).

ing/after the exposure to the video clips [11, 17, 18], and it has been shown that the equilibrium function is affected by the 3D viewing. Especially, the significant influence was obtained from the sway values with the eyes closed after viewing the 3D video clips [17, 18]. Also, it has been elucidated whether the unstability depends on the exposure period. However, it has not been mentioned on remarkable influence while viewing 3D video clips. In this paper, we conducted two types of measurements after resting for 30 seconds: (I) the body sway of each subject was measured for 1 minute with eyes open, and (II) the body sway of each subject was measured for 2 minutes with eyes open. Using the numerical analysis, we examined the 3D viewing effect on our equilibrium function while viewing 3D video clips. Also, we evaluated the rigidity of the postural control system with our numerical analysis.

The previous research showed that the sway values after viewing the 3D video clip are greater than those after viewing the 2D. In this study, the value of the area of sway and the total locus length were significantly greater while viewing the video clip (I)-2D and the control compared with those while viewing the video clip (II)-3D ($p < 0.05$). Also, we proposed the mathematical model while viewing the video clips and evaluated the stabilograms by the numerical analysis. In the numerical solution, the area of sway and the total locus length were proportional to the product $\mu \times \Delta t^*$. In this paper, when Δt^* was around 0.019 and μ was around 3.9 showed close to the actual measurement value of the area of sway and total locus length. The rigidity of the postural control system was the smallest while viewing the video clip (II)-3D. A flexible system to control body sway reduces the product of $\mu \times \Delta t$. Fine postural control, which has been regarded as an anomalous system to control the upright posture, might be seen before the outbreak of motion sickness. This anomalous process is considered to be a clue to elucidating the procedure of the motion sickness and predicting the time when the first symptom of motion sickness will appear.

In the future, we will extend the viewing period of video clips and use the subjective questionnaire to examine the relationship between the VIMS and the body sway. Also, based on the numerical analysis of stabilograms, it was possible to evaluate postural control that could not be seen with the area of sway and total locus length. Using a mathematical model for the evaluation of the stabilograms may contribute to the elucidation of the postural control system.

References

[1] Suyama, S., Date, M. and Takada, H. (2000) Three dimensional display system with dual frequency liquid crystal varifocal lens, *Jpn. J. Appl. Phys.*, **39**, 480–484.

[2] Gabor, D. (1948) A new microscopic principle, *Nature*, **161**, 777–779.

[3] Hatada, T. (1988) *Nikkei electronics*, **444**, 205–223.

[4] Sumio, Y. and Shinji, I. (2001) Visual comfort and fatigue based on accommodation response for stereoscopic image, *The Institute of Image Information and Television Engineers*, **55**(5), 711–717.

[5] Reason, J. T. and Brand, J. J. (1975) *Motion Sickness*, Academic Press, London.

[6] Okawa, T., Tokita, T., Shibata, Y., Ogawa, T. and Miyata, H. (1995) Stabilometry: Significance of locus length per unit area (L/A) in patients with equilibrium disturbances, *Equilib. Res.*, **55**(3), 283–293.

[7] Barmack, N. H. (2003) Central vestibular system: Vestibular nuclei and posterior cerebellum, *Brain Res. Bull.*, **60**, 511–541.

[8] Japan Society for Equilibrium Research (1983) Standard of stabilometry, *Equilib. Res.*, **42**, 367–369.

[9] Kaptyen, T. S., Bles, W., Njiokiktjien, Ch. J., Kodde, L., Massen, C. H. and Mol, J. M. (1983) Standarization in platform stabilometry being a part of posturography, *Agreessologie*, **24**, 321–326.

[10] Hase, M. and Ohta, Y. (2006) Meaning of barycentric position and measurement method, *J. of Environ. Eng.*, **8**, 220–221.

[11] Yoshikawa, K., Kinoshita, F., Miyashita, K., Sugiura, A., Kojima, T., Takada, H. and Miyao, M. (2015) in *Effects of Two-Minute Stereoscopic Viewing on Human Balance Function* (eds. M. Antona and C. Stephanidis), UAHCI/HCII 2015 Part II. LNCS, **9176**, 297–304.

[12] Goldie, P. A., Bach, T. M. and Evans, O. M. (1986) Force platform measures for evaluating postural control: reliability and validity, *Arch. Phys. Med. Rehabil.*, **70**, 510–517.

[13] Emmerrik, R. E. A., Sprague, R. L. V. and Newell, K. M. (1993) Assessment of sway dynamics in tardive dyskinesia and developmental disability, sway profile orientation and stereotypy, *Moving Dis.*, **8**, 305–314.

[14] Collins, J. J. and De Luca, C. J. (1993) Open-loop and closed-loop control of posture: A random-walk analysis of center of pressure trajectories, *Exp. Brain Res.*, **95**, 308–318.

[15] Newell, K. M., Slobounov, S. M., Slobounova, E. S. and Molenaar, P. C. (1997) Stochastic processes in postural center of pressure profiles, *Exp. Brain Res.*, **113**, 158–164.

[16] Takada, H., Kitaoka, Y. and Shimizu, Y. (2001) Mathematicha index and model in stabilometry, *Forma*, **16**, 17–46.

[17] Takada, M., Fukui, Y., Matsuura, Y., Sato, M. and Takada, H. (2015) Peripheral viewing during exposure to a 2D/3D video clip: Effects on the human body, *Environ Health Prev Med.*, **20**, 79–89.

[18] Kinoshita, F., Iwata, K., Matsuura, Y., Miyao, M. and Takada, H. (2016) in *Changes of Potential Functions while Maintaining Upright Postures after Exposure to Stereoscopic Video Clips* (eds. M. Antona and C. Stephanidis), UAHCI 2016, Part II, LNCS, **9738**, 279–286.